

# Limits on Primordial Black Holes from M87

Joseph Silk

Institut d'Astrophysique de Paris, UMR7095:CNRS  
UPMC-Sorbonne University, F-75014, Paris, France

Leo Stodolsky

Max-Planck-Institut für Physik (Werner-Heisenberg-Institut)  
Föhringer Ring 6, 80805 München, Germany

February 14, 2022

## Abstract

Primordial black holes in the solar mass range are a possibly significant component of dark matter. We show how an argument relating the deflection of light by such black holes in the density spike likely to exist around the M87 supermassive black hole, combined with the high resolution observations of the EHT Collaboration, can lead to strong limits on the primordial black hole mass fraction in an astrophysically relevant mass range. The results depend on the model assumed for the dark matter spike and suggest the interest of further understanding of such spikes as well as further high resolution observations on supermassive black holes.

## 1 Introduction

Ascertaining the nature of dark matter remains one of the outstanding problems in cosmology. In recent times there have been active discussions of primordial black holes (PBH's) as a possible dark matter candidate or as a component thereof. These discussions are motivated both by the standard Lambda Cold Dark Matter (LCDM) model of cosmology, which can plausibly generate PBHs in abundance, and by the absence of any need to postulate new physics in order to establish their existence [1].

There have been numerous studies that constrain the mass range of primordial black holes as a significant contributor to dark matter. These include gravitational microlensing [2] and ultrafaint dwarf galaxy heating [3]. However none of these limits are conclusive, either because of the effects of PBH clustering or because of uncertainties in dwarf galaxy dynamical modelling [4]. Indeed, it has equally been argued that the core/cusp transition in dwarfs may be due to PBH heating of cold dark matter [5]. Here we consider a new limit that enables us to set independent constraints on the fraction of asteroid to subsolar

or even solar mass PBHs that can currently be a significant dark matter (DM) contributor.

## 2 Limits on resolution due to black holes

If there is a high density of black holes in some region of space the gravitational fields will be ‘lumpy’ at short distances, inducing random deflections of light rays. These deflections lead to a limitation on the angular resolution possible in observations, and if a high resolution is exhibited in some observation, there is then a limit on the presence of black holes along the flight path. In ref [6] this effect was considered for rays originating from the cosmic microwave background (CMB) and in ref [7] a related, potentially more sensitive method, applicable even when there are no small angle features to observe, was suggested in terms of the loss of coherence between the arms of an interferometer,

However, for the application presented here, the first method, in terms of the angular resolution, is the more favorable. The relevant formula for the limit [6] on the possible angular resolution  $\delta\alpha_{lim}$  for rays passing through a column density of dark matter  $\Sigma$  is

$$(\delta\alpha_{lim})^2 \approx 5 \times 10^{-2} (M/M_\odot) \Sigma_{ly} = 5 \times 10^{-3} (M/M_\odot) \Sigma_{pc}, \quad (1)$$

where the dark matter is composed of black holes of mass  $M$ . The angle  $\delta\alpha_{lim}$  is in  $\mu\text{arcsec}$  and  $\Sigma$  on the right is in terms of solar masses per  $\text{pc}^2$ , as we will use in the following.

Eq 1 is based on the reasoning that if a photon has a high probability, approaching one, of being scattered by a certain angle or more during its flight, then an angular resolution of this amount is not possible. The probability of such a scattering is found from the product of the column density with the cross-section corresponding to the formula  $\delta\alpha = 2r_s/b$  ( $r_s$ =Schwarzschild radius =  $2GM/c^2$ ,  $b$  is impact parameter of the photon,  $c = 1$  units), as in the bending of light by the sun.

A situation combining very high resolution observations with a suspected high density of dark matter arises for the Super Massive Black Hole (SMBH) in the galaxy M87. The EHT collaboration has studied this object with a resolution of  $10 \mu\text{arcsec}$  [8]. At the same time it is likely [9] that a SMBH is surrounded by a ‘spike’ of dark matter. In the present note, we would like to consider the implications of Eq 1 in this situation.

## 3 Models around SMBHs: M87

To estimate  $\Sigma$ , a knowledge of the spike density profile is necessary. This profile is generated by adiabatic growth of the SMBH at early epochs. Its slope however depends on the growth history.

We consider two alternative density profiles. One is  $\rho \propto r^{-7/3}$  for adiabatic growth of the SMBH by gas accretion or stellar tidal disruption. The ambient cold dark matter responds adiabatically and develops a density spike in the

zone of influence of the SMBH. For the present considerations, the dark matter specifically consists of primordial black holes, over what we find to be an astrophysically relevant mass range.

A more conservative case appeals to dynamical relaxation of the accreted dark matter. This would occur after a major merger, although adiabatic growth should eventually resume. In this case,  $\rho \propto r^{-3/2}$  for a black hole merging scenario [10]. A 3/2 profile also results from primordial black hole scattering off of a nuclear star cluster [11].

For the model, we also need the radius  $r_{spike}$  where the density spike begins, within the radius of gravitational influence of the central supermassive black hole, defined by the competition between SMBH gravity and the central stellar velocity dispersion of M87. The spike radius can be defined as [9] the radius where the potential of the SMBH falls to that of the inner galaxy, as inferred from the stellar velocity dispersion via virial arguments. One then has  $r_{spike} = GM_{SMBH}/\sigma_*^2$ , where the black hole mass in M87 is [8]  $M_{SMBH} = 6.5 \pm 0.7 \times 10^9 M_\odot$  and the central stellar velocity dispersion [12] is (with our estimated error from reported long slit absorption spectroscopy)  $\sigma_* = 400 \pm 40$  km/s. We thus take  $r_{spike} = 200$  pc.

### 3.1 Normalization of the spike

In addition to the density profile, we also need to evaluate the absolute size or normalization of the spike. This can be represented by the value of the density at  $r_{spike}$ , which we call  $\rho_{spike}$ . This can then be extrapolated according to the assumed power law to find  $\rho_{horizon}$  as needed in Eq 7 below.

We assume a certain mass for the spike and relate this to  $\rho_{spike}$ . Integrating the power law, one finds

$$M_{spike} \approx 4\pi\rho_{spike}r_{spike}^3 \frac{1}{3-n}, \quad (2)$$

where  $n$  is the power in the profile. One notes that this, as opposed to the integral for  $\Sigma$  below, is essentially independent of  $n$ . This is because when  $\rho$  is not too singular,  $n < 3$ , the geometric factor  $r^2$  in the integral makes it depend essentially on the outer scale.

To proceed, we parameterize the spike mass in terms of a constant  $\eta$  as

$$M_{spike} = \eta \times 1 \times 10^9 M_\odot, \quad (3)$$

so that  $\eta = 1$  would correspond to  $M_{spike}/M_{SMBH} = 0.16$  for M87.. The observed value of  $\rho_{spike}$  can be inferred from the central kinematics of M87 [13] to approximately constrain  $\eta \sim 0.1$ .

We thus write

$$\rho_{spike} = \frac{(3-n)}{4\pi} \frac{1}{r_{spike}^3} M_{spike} = \eta \times 3 \times 10^1 (1-n/3) M_\odot / \text{pc}^3. \quad (4)$$

We record these values for  $\rho_{spike}$  in the second column of the Table. The third column gives the density scaled by the respective power laws to  $r_{horizon} =$

0.001 pc and the fourth column the resulting column density according to Eq 7 below.

### 3.2 Surface density through the “spike”

The column or surface density  $\Sigma$  is given by the integral of the ordinary density  $\rho$  along the flight path:  $\Sigma = \int \rho(r)dr$ . Although the integral should in principle be taken over the entire flight path, it will be dominated by the ‘spike’ and so we estimate it simply from the beginning of the spike,  $r_{spike}$  to the vicinity of the SMBH,  $r_{horizon}$ . We take the inner spike radius  $r_{horizon} = 0.001$  pc from general relativistic studies of the spike for Schwarzschild [14] or Kerr [15] black holes.

Thus

$$\Sigma \approx \int_{r_{spike}}^{r_{horizon}} \rho(r)dr \quad (5)$$

With  $\rho$  represented by the power law  $\rho \sim r^{-n}$  we introduce the rescaled radius  $x = r/r_{horizon}$ . Normalizing to the value at the horizon, we can write

$$\rho = \rho_{horizon} \frac{1}{x^n}. \quad (6)$$

The value of  $\rho_{horizon}$  can be found by magnifying the ambient dark matter density at the beginning of the spike by the factor  $(r_{spike}/r_{horizon})^n$ . It is this large factor which can make the spikes significant in the calculation of a column density. We now carry out the integral Eq 5 in the limit  $(r_{horizon}/r_{spike}) \ll 1$ .

$$\begin{aligned} \Sigma &= r_{horizon} \times \rho_{horizon} \int_1^{(r_{spike}/r_{horizon})} \frac{1}{x^n} dx \\ &= \left(\frac{1}{n-1}\right) r_{horizon} \times \rho_{horizon} (1 - (r_{horizon}/r_{spike})^{n-1}) \\ &\approx \left(\frac{1}{n-1}\right) r_{horizon} \times \rho_{horizon}. \end{aligned} \quad (7)$$

The resulting values for  $\Sigma$  are shown in the last column of the Table.

## 4 Application of EHT resolution of 10 $\mu$ arcsec

With these estimates for  $\Sigma$ , we can apply Eq 1 using the resolution of 10  $\mu$ arcsec stated by the EHT collaboration [8]. Inserting 10  $\mu$ arcsec on the lhs of Eq 1 and requiring that the rhs not exceed this, one finds, with  $\Sigma$  in units of  $M_{\odot}/pc^2$

$$\Sigma \times (M/M_{\odot}) < 2 \times 10^4 \quad (8)$$

The possibility is commonly entertained that the dark matter is composed only partially of primordial black holes, characterized as a fraction  $f_{bh}$  of the total dark matter mass.

Model	$\rho_{spike}$	$\rho_{horizon}$	$\Sigma$
$\rho \sim r^{-3/2}$	$\eta \times 15$	$\eta \times 1 \times 10^9$	$\eta \times 3 \times 10^6$
$\rho \sim r^{-7/3}$	$\eta \times 6.5$	$\eta \times 2 \times 10^{13}$	$\eta \times 1 \times 10^{10}$

Table 1: Parameters for two models of the dark matter spike at the SMBH of M87. The beginning of the spike,  $r_{spike}$ , has been taken to be  $200pc$  from the black hole and its inner radius  $r_{horizon}$  near the SMBH’s horizon, namely  $0.001pc$ . The parameter  $\eta$  characterizes the mass in the spike via Eq 3. The units of the dark matter density  $\rho$  are  $M_{\odot}/pc^3$  and the units of the column or surface density  $\Sigma$  are  $M_{\odot}/pc^2$ .

In the present case, we should then use a column density reduced by  $f_{bh}$ . Since the dark matter mass enters linearly everywhere, one could effect this, for example, by making the replacement  $\eta \rightarrow \eta \times f_{bh}$  in the formulae. Using the inferred value of  $\Sigma$  for the two models, one has the limits

$$\begin{aligned}
 M \times f_{pbh} &\leq \frac{1}{\eta} \times 7 \times 10^{-3} M_{\odot} & \rho \sim r^{-3/2} \text{ model} & \quad (9) \\
 M \times f_{pbh} &\leq \frac{1}{\eta} \times 2 \times 10^{-6} M_{\odot} & \rho \sim r^{-7/3} \text{ model} &
 \end{aligned}$$

These limits should apply regardless of the possible clustering of primordial black holes. Clusters would not survive within the density spike around the SMBH. Poisson fluctuation-induced clustering has been shown to greatly reduce the number of predicted merger events [16], and allows the resurrection of a significant solar mass component of PBHs that could account for the observed LIGO/VIRGO black hole merger rates [17]. The astrophysical and primordial black hole interpretationa are currently indistinguishable [18]. Our results show the possibiity for strong limits on compact objects by a new independent method. In particular the second variant in Eq 9 is of interest for the asteroid/earth mass range. This can be compared with the results of the OGLE [19] and Subaru [20] microlensing collaborations. The M31 microlensing data, revised for finite lens size effects [21], sets a limit of around 1% on the mass fraction of PBHs contributing to dark matter in the mass range  $10^{-9} - 10^{-6} M_{\odot}$ .

## 5 Comparisons

A number of other methods have been used to limit the possibilities for primordial black holes . In Fig1 we show some representative limits, in the  $(M/M_{\odot}, f_{pbh})$  plane, as compared to ours from Eq 9. We show the case  $\eta = 0.1$ . The dashed (right) line is for the  $\rho \sim r^{-3/2}$  model and the solid (left) line is for the  $\rho \sim r^{-7/3}$  model. The excluded region, according to Eq 9, lies to the right and above these lines.

Our arguments appear to exclude a considerable region of the right-hand part of the  $(M/M_\odot, f_{pbh})$  plane, in agreement with, and with the  $\rho \sim r^{-7/3}$  model, extending previous exclusions. On the other hand, in the limiting case where the dark matter consists entirely of primordial black holes or  $f_{pbh} = 1$ , the method does not seem to provide limits as strong as those from microlensing. Improvement in the input information, such as higher resolution observations, would tend to move the exclusion lines to the left.

The other exclusion limits shown on the plot have been obtained from reference [1] and from reference [22].

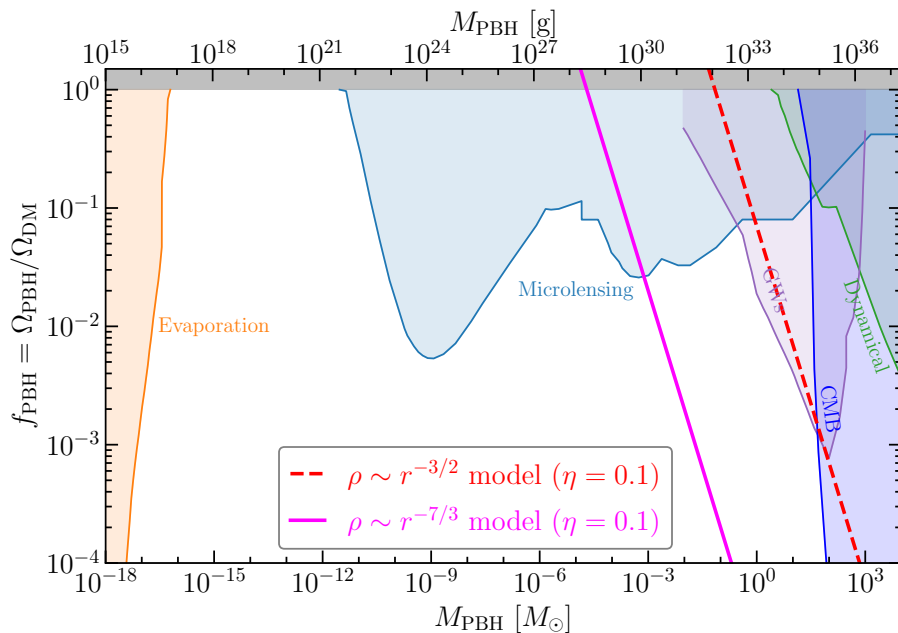


Figure 1: Limits on primordial black holes exhibited in the  $(M/M_\odot, f_{pbh})$  plane, using Eq 9, for the  $\rho \sim r^{-3/2}$  model (dashed, right, line) and for the  $\rho \sim r^{-7/3}$  model (solid, left, line) The respective excluded regions are to the right of these lines. Other limits are quoted from [1] and [22]. Figure graciously provided by Guillem Domenech.

## 6 Interpretation

These interesting limits illustrate the potential power of the method. They arise essentially from the sharpness of the spike, with the associated large values of  $\rho_{horizon}$ . The large difference between the two variants in Eq 9 arises from the sensitivity to the steepness of the spike profile. Thus an improvement in the definition of our results would come from a better understanding of the spike profile,

either by observational or theoretical arguments. Of course, better knowledge of  $M_{spike}$  or even better observational resolution would also be helpful.

As stressed in [6] and [7] the interpretation of a possible positive signal would be a much more subtle matter than the simple setting of limits as we do here. That is, if a loss of, or a limit on, observational resolution is found, all other reasons for this, natural or instrumental, have to be considered before attributing the effect to primordial black holes. Further observations of other SMBH's with high resolution would be of interest in connection with our arguments. Note that in Eq 1 the resolution enters quadratically, and similarly on the rhs of Eq 8, so improved high resolution will have a strong effect on the limits.

It is difficult to avoid the development of a dark matter spike around the SMBH in M87. It may be modulated by SMBH merging, but this would have most likely occurred within the first billion years after SMBH formation. Hence the effective value of accumulated DM mass in the spike could be slightly reduced. We argue that the adiabatic build-up of the central SMBH in massive elliptical galaxies inevitably results in DM spike formation, with intriguing consequences for the EHT observations of the supermassive black hole in M87.

In the event that PBHs form all or most of the DM, an interesting aspect of our method is that any pre-existing clustering of PBHs, such as that invoked to account for consistency with the early MACHO experiments and with the LIGO/VIRGO event rates, would not be preserved in the spike. With improved understanding of spikes and further observations involving them, our new kind of limit promises new, independent constraints on PBH masses as a DM contributor.

## 7 Acknowledgement

We thank Guillem Domenech for providing us with Figure 1.

## References

- [1] Green, A. M., Kavanagh, B. J. 2021. Primordial black holes as a dark matter candidate. *Journal of Physics G Nuclear Physics* 48. 043001 (2021).
- [2] B. Paczynski, Gravitational Microlensing by the Galactic Halo, *Astrophys. J.* **304**, 1 (1986). For limits in the solar mass range, see R. A. Allsman *et al.* [Macho Collaboration], MACHO Project Limits on Black Hole Dark Matter in the 1-30 Solar Mass Range, *Astrophys. J.* **550**, L169 (2001) doi:10.1086/319636 [astro-ph/0011506].
- [3] Lu, P., Takhistov, V., Gelmini, G. B., Hayashi, K., Inoue, Y., Kusenko, A. 2021. Constraining Primordial Black Holes with Dwarf Galaxy Heating. *The Astrophysical Journal* 908, 23 (2021); Stegmann, J., Capelo, P. R., Bortolas, E., Mayer, L. 2020. Improved constraints from ultra-faint dwarf galaxies on primordial black holes as dark matter. *Monthly Notices of*

- the Royal Astronomical Society 492, 5247 P5260; Lu, B.-Q., Wu, Y.-L. 2019. Constraining primordial black holes in dark matter with kinematics of dwarf galaxies. *Physical Review D* 99.123023; Stegmann, J., Capelo, P. R., Bortolas, E., Mayer, L. 2020. Improved constraints from ultra-faint dwarf galaxies on primordial black holes as dark matter. *Monthly Notices of the Royal Astronomical Society* 492, 5247 P5260. Brandt, T. D. 2016. Constraints on MACHO Dark Matter from Compact Stellar Systems in Ultra-faint Dwarf Galaxies. *The Astrophysical Journal* 824, 31
- [4] Zhu, Q., Vasiliev, E., Li, Y., Jing, Y. 2018. Primordial black holes as dark matter: constraints from compact ultra-faint dwarfs. *Monthly Notices of the Royal Astronomical Society* 476, 2P11; García-Bellido, J., Clesse, S. 2018. Constraints from microlensing experiments on clustered primordial black holes. *Physics of the Dark Universe* 19, 144 P148. For a review, see
- [5] Boldrini, P., Miki, Y., Wagner, A. Y., Mohayaee, R., Silk, J., Arbey, A. 2020. Cusp-to-core transition in low-mass dwarf galaxies induced by dynamical heating of cold dark matter by primordial black holes. *Monthly Notices of the Royal Astronomical Society* 492, 5218 P5225.
- [6] Stodolsky, L. 2019. Observational Aspect of Black Hole Dark Matter. *Mod.Phys.Let.* **36 A**, no.11 (2021), arXiv:1912.01325.
- [7] Stodolsky, L. 2021. Primordial Black Holes in Interferometry. arXiv:2105.03648v2
- [8] Event Horizon Telescope Collaboration and 348 colleagues 2019. First M87 Event Horizon Telescope Results. I. The Shadow of the Supermassive Black Hole. *The Astrophysical Journal* 875. doi:10.3847/2041-8213/ab0ec7
- [9] Gondolo, P., Silk, J. 1999. Dark Matter Annihilation at the Galactic Center. *Physical Review Letters* 83, 1719, 1722. doi:10.1103/PhysRevLett.83.1719.
- [10] Merritt, D., Milosavljević, M., Verde, L., Jimenez, R. 2002. Dark Matter Spikes and Annihilation Radiation from the Galactic Center. *Physical Review Letters* 88. doi:10.1103/PhysRevLett.88.191301
- [11] O. Y. Gnedin and J. R. Primack, “Dark Matter Profile in the Galactic Center,” *Phys. Rev. Lett.* **93**, 061302 (2004) doi:10.1103/PhysRevLett.93.061302 [arXiv:astro-ph/0308385 [astro-ph]].
- [12] Longobardi, A., Arnaboldi, M., Gerhard, O., Pulsoni, C., Söldner-Rembold, I. 2018. Kinematics of the outer halo of M 87 as mapped by planetary nebulae. *Astronomy and Astrophysics* 620. doi:10.1051/0004-6361/201832729
- [13] Murphy, J. D., Gebhardt, K., Adams, J. J. 2011. Galaxy Kinematics with VIRUS-P: The Dark Matter Halo of M87. *The Astrophysical Journal* 729. doi:10.1088/0004-637X/729/2/129; arXiv:1101.1957.



- [14] Sadeghian, L., Ferrer, F., Will, C. M. 2013. Dark-matter distributions around massive black holes: A general relativistic analysis. *Physical Review D* 88. doi:10.1103/PhysRevD.88.063522
- [15] F. Ferrer, A. M. da Rosa and C. M. Will, “Dark matter spikes in the vicinity of Kerr black holes,” *Phys. Rev. D* **96**, no.8, 083014 (2017) doi:10.1103/PhysRevD.96.083014 [arXiv:1707.06302 [astro-ph.CO]].
- [16] 2021PhRvL.126e1302J Jedamzik, K. 2021. Consistency of Primordial Black Hole Dark Matter with LIGO/Virgo Merger Rates. *Physical Review Letters* 126. doi:10.1103/PhysRevLett.126.051302
- [17] Clesse, S., Garcia-Bellido, J. 2020. GW190425, GW190521 and GW190814: Three candidate mergers of primordial black holes from the QCD epoch. arXiv e-prints. arXiv:2007.06481
- [18] Franciolini, G. and 8 colleagues 2021. Quantifying the evidence for primordial black holes in LIGO/Virgo gravitational-wave data. arXiv:2105.03349
- [19] H. Niikura, M. Takada, S. Yokoyama, T. Sumi and S. Masaki, Constraints on Earth-mass primordial black holes from OGLE 5-year microlensing events, *Phys. Rev. D* **99**, no.8, 083503 (2019) doi:10.1103/PhysRevD.99.083503 [arXiv:1901.07120 [astro-ph.CO]].
- [20] H. Niikura, M. Takada, N. Yasuda, R. H. Lupton, T. Sumi, S. More, T. Kurita, S. Sugiyama, A. More and M. Oguri, *et al.* Microlensing constraints on primordial black holes with Subaru/HSC Andromeda observations, *Nature Astron.* **3**, no.6, 524-534 (2019) doi:10.1038/s41550-019-0723-1 [arXiv:1701.02151 [astro-ph.CO]].
- [21] Smyth, N., Profumo, S., English, S., Jeltama, T., McKinnon, K., Guhathakurta, P. 2020. Updated constraints on asteroid-mass primordial black holes as dark matter. *Physical Review D* 101. doi:10.1103/PhysRevD.101.063005
- [22] B, J, Kavanagh, PBH Bounds, version 1.0, Zenodo 2019, doi:10.5281/zenodo.3538999